Dalton Transactions

ROYAL SOCIETY OF CHEMISTRY

COMMUNICATION

View Article Online
View Journal | View Issue

Cite this: *Dalton Trans.*, 2023, **52**, 7787

Received 20th April 2023,
Accepted 26th May 2023

DOI: 10.1039/d3dt01188g

rsc.li/dalton

Cyclometalated platinum(II) complex as a selective light switch for G-quadruplex DNA†

Meenaxi Saini and Tia E. Keyes *

Cyclometalated 1,3-bis(8-quinolyl) phenyl chloroplatinum(II) (Pt1) shows selective luminescence transduction of G-quadruplex binding over duplex DNA. The effect is enhanced on association with parallel and hybrid G-quadruplex structures over other topologies. The kinetics of binding are studied for c-myc and the response is found to be partially reversible in a displacement assay.

G-quadruplexes (G4) are non-canonical nucleic acid structures formed in guanine-rich regions of both DNA and RNA *in vivo*, by self-assembly of four guanines *via* Hoogsteen hydrogen bonds.[1] G4 structures form a number of topologies depending on the orientation of DNA strands including parallel, antiparallel, hybrid, and they may be intramolecular (formed through a single strand) or intermolecular (from multiple strands). They can also adopt various loop structures.[1–3] The biological role of G4 structures is still emerging, but their importance in telomerase maintenance and regulation of gene expression, is well established and their role in cancer/oncogenes makes them particularly compelling both as therapeutic and diagnostic targets.[4,5]

Transition metal complexes are increasingly studied as small molecule ligands for G4.[6–8] Amongst these, Pt(II) complexes, have been fairly widely explored as their square planar structures offer a flattened geometry that can promote binding to G4 structures through π-stacking/end-capping compared to the octahedra of Ruthenium and Rhenium which have been more widely studied in duplex DNA binding.[9–13] Terpyridine complexes, particularly those with labile Cl ligands, such as 4′-tolyl-2,2′:6′,2″-terpyridine Pt(II) chloride have been shown to have high binding affinity and specificity toward G-quadruplex[14,15] and, end capping has been reported to be accompanied by platination of adenine loop sites on some G-quadruplex structures.[16,17] Other non-covalent binding modes such as groove binding, electrostatic association and hydrogen bonding interactions can also occur and a number of Pt(II) complexes show more than one mode of interaction with G4s.[17]

Cyclometalated platinum(II) complexes bearing π-conjugated organic ligands have been much less widely studied in the context of G quadruplex binding than N-coordinated analogues.[18–24] Although for tridentate ligand coordinated complexes they have advantageous photophysical properties that have been exploited across a range of domains,[25–28] including as probes for biomolecules[29] and bioimaging.[30–33] Given their structural analogy to N,N,N Pt terpy complexes we rationalised they might be expected to show similar affinity but with superior addressability due to their photophysical properties in terms of both luminescent quantum yield and red emission wavelength.[34,35] In particular, we are interested in G4 ligands that show molecular light switch properties, with weak/no emission from aqueous media that switches on, on target binding. Such behaviour has been widely observed in ruthenium complexes containing phenazine ligands.[36,37] Rarer in Pt complexes,[38] it has been noted in Pt(II) benzimidazole N,N,N complex on aggregation on binding to RNA[39] and in Pt terpy complexes with an appended fluorophore.[40] Kinetic control for Pt binding with G4 was reported very recently.[41] Herein, we show that cyclometalated tridentate Pt complex 1,3-bis(8-quinolyl) phenyl chloroplatinum(II) (**Pt1**), under visible excitation, shows dramatic changes in emission amplitude and selective signal transduction of G quadruplex binding with sharp discrimination in behaviour between G4s and duplex DNA (Fig. 1).

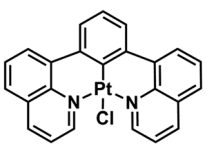

Fig. 1 Chemical structure of **Pt1**.

School of Chemical Science and National Centre for Sensor Research Dublin City University, Dublin 9, Ireland. E-mail: tia.keyes@dcu.ie

† Electronic supplementary information (ESI) available. See DOI: https://doi.org/10.1039/d3dt01188g

1,3-Bis(8-quinolyl) phenyl chloroplatinum(II) (**Pt1**) was prepared as reported by Williams *et al.* and structural analysis and photophysical properties conformed to their reported data.[42] In aqueous PBS/KCl buffer at pH 7.0, **Pt1** shows an absorbance feature at λ_{max} ~ 420 nm (Fig. S1†) attributed to d(Pt)/π(Cl) → π*(ligand) transition.[42] Excitation at this wavelength results in intense luminescence in non-protic solvent (*e.g.* λ_{em} 600 nm, lifetime 865 ns in deaerated DMSO) (Fig. S2†) that is substantially and reversibly extinguished on titration with water (Fig S8†). In aerated aqueous PBS/KCl buffer at pH 7.0, emission is weak and short lived with an emission lifetime of 2 ns (~99% amplitude) in aerated buffer (Fig. 2, Table S1†).

We compared **Pt1** association across four G-rich oligonucleotides known to assemble into different representative G4 topologies: c-mycT and 21 KRAS form parallel G4, TBA forms antiparallel, 22 AG forms mix-hybrid and Inter G4 that forms an intermolecular G quadruplex structures. Binding was also compared with ct-DNA and short oligomer ds17A as representative duplex structures (full sequences are provided in ESI†). The impact of **Pt1** incubation with c-mycT on its electronic spectroscopy is shown in Fig. 2A, where the d(Pt)/π(Cl) → π* (ligand) absorbance at 420 nm showed time-dependent hypochromicity in PBS/KCl buffer, shifting to approximately 406 nm with roughly 50% decrease in intensity. Such extensive change suggests Cl^- loss on G4 association.[15,23] Similar shifts in absorbance were seen on KRAS and 22AG association though without comparable loss in absorbance intensity (Fig. S3 and S4†). By contrast, absorbance changes for the other quadruplexes were modest (Fig. S5 and S6†), and with duplex (ct) DNA and duplex DNA oligomer ds17A (Fig. 2C and Fig. S7†) changes to absorbance were negligible.

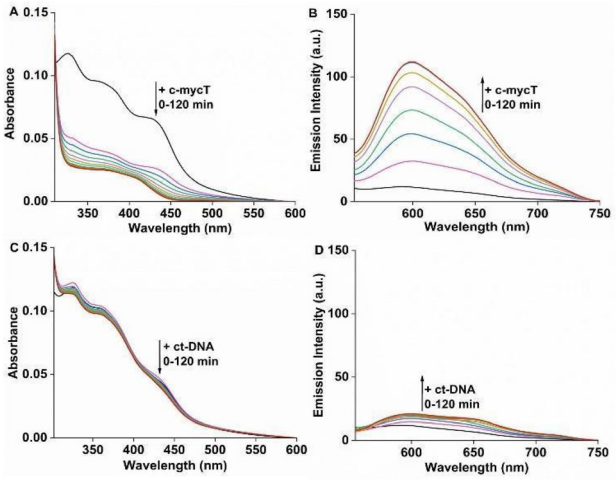

Fig. 2 (A) Change in absorbance and (B) emission spectra of **Pt1** complex (10 μM) in PBS/KCl buffer pH 7.0 with 30 μM c-mycT (c-mycT/Pt = 3) from 0 minute (black line) up to saturation (red, 120 minutes). (C and D) change in absorbance and emission of **Pt1** complex in PBS/KCl buffer pH 7.0 with 100 μM ct-DNA (ct-DNA/Pt = 10) from 0 minute (black line) up to saturation (red, 120 minutes) respectively. λ_{ex} = 420 nm.

Fig. 2B shows the time-dependent evolution of emission signal on incubation of **Pt1** in aqueous media (PBS/KCl buffer, pH 7.0) with 3 molar equivalents of c-mycT. Both the magnitude of emission intensity change at saturation, and the rate (or indeed presence at all) of dynamic response were G4 topology dependent. The most dramatic response was observed on c-mycT association, where compared to aqueous buffer, emission increased approx. 14-fold on G4 association, yielding an emission quantum yield that exceeds that of the complex in non-aqueous media. A red shift of emission maxima by approx. 12 nm and alteration to the emission profile accompany the intensity change. Compensating for the large decrease in absorbance cross-section of the complex on c-mycT binding, the emission intensity increase is actually nearly 30-fold. KRAS and 22AG induced less dramatic, but nonetheless large increases in emission intensity (Fig. 3), of close to an order of magnitude on **Pt1** binding compared to buffer.

TBA and Int G4 association induced much weaker emission responses, where intensity increased approximately 4-fold compared to complex in buffer. For duplex DNA; ct-DNA and DNA oligomer ds17A, emission intensity changes were very weak (Fig. 2D and Fig. S7†). The final intensity increased less than 2-fold over complex in buffer solution. And, for TBA, Int G4 and duplex, intensity showed little time dependence. The addition of further concentrations of G4/duplex in each case did not alter the emission spectra further (Fig. S9†). The emission intensity changes were accompanied by increases to emission lifetime (Fig. S10 and Table S1†). Emission lifetime increased from predominantly 2 ns in aerated buffer to approximately 318 ns on association with duplex DNA, TBA or Int G4 whereas on binding to c-mycT emission lifetime was dramatically extended to 486 ns and to 424 ns and 351 ns for KRAS and 22AG respectively. Overall, there is clear distinction in signal transduction for both spectroscopic and photophysical data between **Pt1** interaction with parallel and mixed hybrid quadruplexes showing enhanced emission compared to

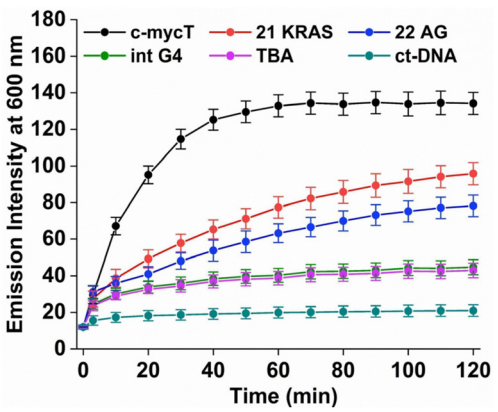

Fig. 3 Temporal evolution of emission signal at λ_{max} 600 nm of 10 μM **Pt1** in PBS/KCl buffer pH 7.0 on addition of 30 μM G-quadruplexes [G-quadruplex/**Pt1** = 3] and 100 μM ct-DNA. Emission intensities are not corrected for absorbance changes. λ_{ex} = 420 nm.

antiparallel, intermolecular quadruplex topology or to duplex DNA.

The binding constants for G4s and ctDNA were estimated from concentration-dependent emission intensity plots taken from time-equilibrated data (after 2 hours of equilibration). K_b for c-mycT was determined as $(1.8 \pm 0.2) \times 10^5$ M^{-1}.[43,44] The stoichiometry of binding for **Pt1** – c-mycT G4 interaction was determined from Jobs plot as approximately 2 : 1 (Fig. S12†). The K_b of **Pt1** were determined as $(1.2 \pm 0.1) \times 10^5$ M^{-1}, $(0.8 \pm 0.06) \times 10^5$ M^{-1} for KRAS and 22 AG respectively, which are of the same order of magnitude as c-mycT. However, for duplex and the remaining quadruplex structures, binding was too weak to accurately determine (Table S1†). Therefore, **Pt1** complex shows the greatest affinity for parallel and hybrid quadruplex with good selectivity over other topologies (Table S1†), including duplex DNA. The difference in binding affinities of the **Pt1** complex for different quadruplex structures is presumably driven by differences in the loop structure and topology of quadruplex. A case in point is the variation in the binding affinity between c-mycT and KRAS. Both have parallel structures, confirmed from CD spectroscopy, with the same strand orientation and both comprise three quartets, but their loop structures are different. KRAS exhibits three regular propeller loops but c-mycT promoter P1, one of seven nuclease-hypersensitive elements (NHEs), NHE III1 of c-mycT gene, has been shown to provides unusual fold-back configuration and reversal loops which connect the G-tetrad layers, which are likely responsible for the variation in binding affinity.[45,46]

However, the time dependence of the emission response for c-mycT, KRAS and 22AG, and the absence of such kinetic effects for the duplex, TBA and Int, are consistent with weak and non-covalent association in the latter three cases and may indicate covalent association in the former. By fitting the 600 nm intensity plots *versus* time to a pseudo first order rate equation ($\Delta I = A(1 - \exp(-kt)$, where A is constant and k is observed reaction rate constant) for **Pt1** interaction with c-mycT, KRAS and 22 AG, we obtained values of 0.066 ± 0.004 min^{-1}, 0.021 ± 0.002 min^{-1}, 0.019 ± 0.002 min^{-1} respectively for each G4 (Fig. S13†).

Again, it is notable that both affinity and observed rate constant is greatest for c-mycT. The analogous, N,N,N coordinated Pt TerpyCl complex has been reported to associate to the tetrad by terminus stacking as well as through coordination to adenine in G4 quadruplex. The clear distinction in behaviour between G4 topologies and duplex here, may be attributed to this same effect. The only site of adenine in the c-mycT is at the terminal of the sequence, so if adenine binding facilitates G4 interaction, one would expect replacement of adenine with thiamine to reduce the affinity and emission intensity of the associated complex. Therefore, to evaluate the potential role of adenine platination in emission enhancement, **Pt1** solution was incubated with 3 molar equivalents of c-mycTT (where both adenines at 3′ terminus of c-mycT sequence are replaced by thymine). CD spectroscopy confirmed the fold was the same as c-mycT. However, the emission intensity increased only 6-fold compared to the complex in aqueous buffer (Fig. S14†) *i.e.* to only half the emission enhancement observed on c-mycT binding. These results strongly implicate the contribution of adenine platination to emission enhancement. Incubating the complex in buffer with adenine monophosphate alone, lead to only modest increases in emission enhancement (roughly 16% increase) so the effect is likely cooperative whereby adenine binding facilitates stronger non-specific interaction with the c-mycT G4 structure that maximizes its emission enhancement.

To further confirm the G4 structure is responsible for the emission enhancement, we carried out titrations of **Pt1** against c-mycT in the presence of Li^+ which is not expected to stabilise the G4.[47,48] Correspondingly, the changes in emission intensity observed were similar to duplex DNA (Fig. S11†) indicating the Li+ is not stabilising the structure and that the response arises specifically from the G4 structure.

Finally, to evaluate the effect of conjugate binding on G4 DNA conformation, circular dichroism (CD) spectra were measured across different ratios of **Pt1** to G4 DNA. The CD spectrum of c-mycT gave the expected negative band at 245 nm and a positive feature at 265 nm (Fig. S15†) characteristic of a predominantly parallel structure.[49]

With increasing concentration of **Pt1** complex, Fig. 4A a positive induced CD (ICD) feature appeared at 420 nm, attributed to π-stacking at the tetrad terminal accompanied by adenine platination.[16,17] The small change in molar ellipticity of the quadruplex (about 18% increase) at 245 nm and 265 nm indicates that **Pt1** stabilises the quadruplex. Similar CD spectral changes were observed for 21 KRAS with increasing concentration of **Pt1** (Fig. S16†).

Finally, a fluorescence displacement study was performed by adding Phen-DC3 to the c-mycT-**Pt1** complex after it had been allowed to assemble for 2 hours. Phen-DC3 is a selective G4 binder with high affinity for G4 quadruplex.[50] As shown in Fig. 4B addition of Phen-DC3 results in a progressive reduction in the emission intensity of the c-mycT-**Pt1** complex and the response saturates at 100 μM of Phen-DC3. Notably, the final emission intensity remains relatively higher than the **Pt1** complex in buffer solution with a 3-fold decrease in intensity indicating the displacement of **Pt1** with Phen-DC3 is incomplete. NMR spectroscopy studies suggested that Phen-DC3

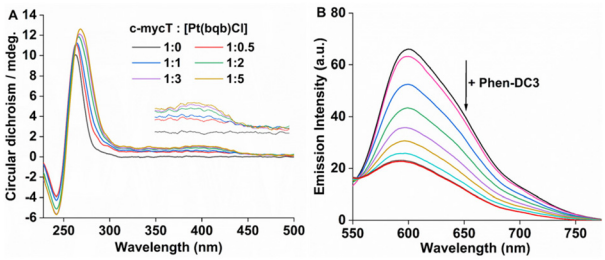

Fig. 4 (A) Changes to the CD spectrum of c-mycT with increasing **Pt1** concentration in PBS/KCl pH 7.0. (B) Changes to the emission spectra of **Pt1** 5 μM incubated with 15 μM c-mycT [c-mycT/**Pt1** = 3] on addition of 5 μM to 100 μM Phen-DC3 (PBS/KCl pH.7.0).

associates with the guanine base of the top G-tetrad in G-quadruplex *via* extensive π-stacking.[51] Reduction in the emission intensity of the c-mycT-**Pt1** complex with the addition of Phen-DC3 also suggests both ligands (**Pt1** and Phen-DC3) occupy similar binding sites on the quadruplex consistent with π-stacking interaction of **Pt1** complex at terminal tetrad of G-quadruplex.

In summary, cyclometalated Pt complex; 1,3-bis(8-quinolyl) phenyl chloroplatinum(II) shows outstanding emission signal transduction on binding to adenine containing parallel or hybrid G-quadruplex DNA. Optical and photophysical properties show that association induced changes are much weaker with duplex DNA and antiparallel structures. The data indicate that cooperative non-covalent and covalent platination interactions may be responsible for the effect. CD spectroscopy shows stabilisation of the G4 structure for these three structures, with evidence of induced CD.

Overall, the photophysical data indicate that the quadruplex may be readily distinguished from DNA bound Pt complex with dramatic changes to emission lifetime that may facilitate lifetime imaging as a means to distinguish such structures *in vivo*.

Conflicts of interest

There are no conflicts of interest.

Acknowledgements

This work is supported by Science Foundation Ireland under 19/FFP/6428, 12/RC/2276_P2 and EU.COFUND – Marie Skłodowska-Curie Actions.

References

1 M. L. Bochman, K. Paeschke and V. A. Zakian, *Nat. Rev.*, 2012, **13**, 770–780.
2 T. Zok, N. Kraszewska, J. Miskiewicz, P. Pielacinska, M. Zurkowski and M. Szachniuk, *Nucleic Acids Res.*, 2022, **50**, D253–D258.
3 S. Ceschi, M. Berselli, M. Cozzaglio, M. Giantin, S. Toppo, B. Spolaore and C. Sissi, *Nucleic Acids Res.*, 2022, **50**, 1370–1381.
4 S. Pramanik, Y. Chen, H. Song, I. Khutsishvili, L. A. Marky, S. Ray, A. Natarajan, P. K. Singh and K. K. Bhakat, *Nucleic Acids Res.*, 2022, **50**, 3394–3412.
5 J. T. Grün, A. Blümler, I. Burkhart, J. W. Bartoschek, A. Heckel and H. Schwalbe, *J. Am. Chem. Soc.*, 2021, **143**, 6185–6193.
6 A. Łęczkowska, J. G. Garcia, C. P. Arnaiz, B. Garcia, A. J. P. White and R. Vilar, *Chem. – Eur. J.*, 2018, **24**, 11785–11794.
7 G. Farine, C. Migliore, A. Terenzi, F. L. Celso, A. Santoro, G. Bruno, R. Bonsignore and G. Barone, *Eur. J. Inorg. Chem.*, 2021, 1332–1336.
8 O. Domarco, C. Kieler, C. Pirker, C. Dinhof, B. Englinger, J. M. Reisecker, G. Timelthaler, M. D. Garcia, C. Peinador, B. K. Keppler, W. Berger and A. Terenzi, *Angew. Chem., Int. Ed.*, 2019, **58**, 8007–8012.
9 F. E. Poynton, J. P. Hall, P. M. Keane, C. Schwarz, I. V. Sazanovich, M. Towrie, T. Gunnlaugsson, C. J. Cardin, D. J. Cardin, S. J. Quinn, C. Long and J. M. Kelly, *Chem. Sci.*, 2016, **7**, 3075–3084.
10 J. D. Knoll and C. Turro, *Coord. Chem. Rev.*, 2015, **282**, 110–126.
11 L. Holden, C. S. Burke, D. Cullinane and T. E. Keyes, *RSC Chem. Biol.*, 2021, **2**, 1021–1049.
12 K. T. McQuaid, S. Takahashi, L. Baumgaertner, D. J. Cardin, N. G. Paterson, J. P. Hall, N. Sugimoto and C. J. Cardin, *J. Am. Chem. Soc.*, 2022, **144**, 5956–5964.
13 G. Li, L. Sun, L. Ji and H. Chao, *Dalton Trans.*, 2016, **45**, 13261–13276.
14 E. Morel, C. Beauvineau, D. Naud-Martin, C. Landras-Guetta, D. Verga, D. Ghosh, S. Achelle, F. Mahuteau-Betzer, S. Bombard and M. P. Teulade-Fichou, *Molecules*, 2019, **24**, 404.
15 M. Chrzanowska, A. Katafias, A. Kozakiewicz and R. v. Eldik, *Inorg. Chim. Acta*, 2020, **504**, 119449.
16 H. Bertrand, S. Bombard, D. Monchaud, E. Talbot, A. Guedin, J.-L. Mergny, R. Grunert, P. J. Bednarski and M. P. Teulade-Fichou, *Org. Biomol. Chem.*, 2009, **7**, 2864–2871.
17 M. Trajkovski, E. Morel, F. Hamon, S. Bombard, M. P. Teulade-Fichou and J. Plavec, *Chem. – Eur. J.*, 2015, **21**, 7798–7807.
18 D.-L. Ma, C.-M. Che and S.-C. Yan, *J. Am. Chem. Soc.*, 2009, **131**(5), 1835–1846.
19 T. Kench, P. A. Summers, M. K. Kuimova, J. E. M. Lewis and R. Vilar, *Angew. Chem., Int. Ed.*, 2021, **60**, 10928–10934.
20 P. Wu, D.-L. Ma, C.-H. Leung, S.-C. Yan, N. Zhu, R. Abagyan and C.-M. Che, *Chem. – Eur. J.*, 2009, **15**, 13008–13021.
21 K. Suntharalingam, A. Łęczkowska, M. A. Furrer, Y. Wu, M. K. Kuimova, B. Therrien, A. J. P. White and R. Vilar, *Chem. – Eur. J.*, 2012, **18**, 16277–16282.
22 A. D. Richards and A. Rodger, *Chem. Soc. Rev.*, 2007, **36**, 471–483.
23 A. I. Solomatina, P. S. Chelushkin, T. O. Abakumova, V. A. Zhemkov, M. Kim, I. Bezprozvanny, V. V. Gurzhiy, A. S. Melnikov, Y. A. Anufrikov, I. O. Koshevoy, S.-H. Su, P.-T. Chou and S. P. Tunik, *Inorg. Chem.*, 2019, **58**(1), 204–217.
24 B. S. McGhie, J. Sakoff, J. Gilbert, C. P. Gordon and J. R. Aldrich-Wright, *Int. J. Mol. Sci.*, 2022, **23**, 10469.
25 M. D. Aseman, M. Nikravesh, A. Abbasi and H. R. Shahsavari, *Inorg. Chem.*, 2021, **60**, 18822–18831.
26 E. M. Bolitho, C. S. Cano, H. Shi, P. D. Quinn, M. Harkiolaki, C. Imberti and P. J. Sadler, *J. Am. Chem. Soc.*, 2021, **143**, 20224–20240.

27 D. M. Yufanyi, H. S. Abbo, S. J. J. Titinchi and T. Neville, *Coord. Chem. Rev.*, 2020, **414**, 213285.
28 G. Li, S. Liu, Y. Sun, W. Lou, Y.-F. Yang and Y. She, *J. Mater. Chem. C*, 2022, **10**, 210–218.
29 A. Zamora, E. Wachter, M. Vera, D. K. Heidary, V. Rodríguez, E. Ortega, V. Fernandez-Espín, C. Janiak, E. C. Glazer, G. Barone and J. Ruiz, *Inorg. Chem.*, 2021, **60**, 2178–2187.
30 M. Z. Shafikov, A. F. Suleymanova, R. J. Kutta, A. Gorski, A. Kowalczyk, M. Gapińska, K. Kowalski and R. Czerwieniec, *J. Mater. Chem. C*, 2022, **10**, 5636–5647.
31 W. A. Tarran, G. R. Freeman, L. Murphy, A. M. Benham, R. Kataky and J. A. G. Williams, *Inorg. Chem.*, 2014, **53**, 5738–5749.
32 K.-C. Tong, P.-K. Wan, C.-N. Lok and C.-M. Che, *Chem. Sci.*, 2021, **12**, 15229–15238.
33 D. Septiadi, A. Aliprandi, M. Mauro and L. D. Cola, *RSC Adv.*, 2014, **4**, 25709–25718.
34 D. A. Haque, L. Xu, R. A. Al-Balushi, M. K. Al-Suti, R. Ilmi, Z. Guo, M. S. Khan, W.-Y. Wong and P. R. Raithby, *Chem. Soc. Rev.*, 2019, **48**, 5547–5563.
35 K. Li, G. S. M. Tong, Q. Wan, G. Cheng, W.-Y. Tong, W.-H. Ang, W.-L. Kwong and C.-M. Che, *Chem. Sci.*, 2016, **7**, 1653–1673.
36 S. Shi, J. Zhao, X. Gao, C. Lv, L. Yang, J. Hao, H. Huang, J. Yao, W. Sun, T. Yao and L. Ji, *Dalton Trans.*, 2012, **41**, 5789–5793.
37 C. Rajput, R. Rutkaite, L. Swanson, I. Haq and J. A. Thomas, *Chem. – Eur. J.*, 2006, **12**, 4611–4619.
38 D.-L. Ma, C.-M. Che and S.-C. Yan, *J. Am. Chem. Soc.*, 2009, **131**, 1835–1846.
39 A. S.-Y. Law, L. C.-C. Lee, K. K.-W. Lo and V. W.-W. Yam, *J. Am. Chem. Soc.*, 2021, **143**, 5396–5405.
40 S. Gama, I. Rodrigues, F. Mendes, I. C. Santos, E. Gabano, B. Klejevskaja, J. Gonzalez-Garcia, M. Ravera, R. Vilar and A. Paulo, *J. Inorg. Biochem.*, 2016, **160**, 275–286.
41 B.-C. Zhu, J. He, W. Liu, X.-Y. Xia, L.-Y. Liu, B.-B. Liang, H.-G. Yao, B. Liu, L.-N. Ji and Z.-W. Mao, *Angew. Chem., Int. Ed.*, 2021, **60**, 15340–15343.
42 K. L. Garner, L. F. Parkes, J. D. Piper and J. A. G. Williams, *Inorg. Chem.*, 2010, **49**, 476–487.
43 A. Mitra, S. Bhowmik and R. Ghosh, *J. Photochem. Photobiol.*, 2021, **6**, 100033.
44 T.-P. Sheng, X.-X. Fan, G.-Z. Zheng, F.-R. Dai and Z.-N. Chen, *Molecules*, 2020, **25**, 2656.
45 A. Ou, J. W. Schmidberger, K. A. Wilson, C. W. Evans, J. A. Hargreaves, M. Grigg, M. L. O'Mara, K. S. Iyer, C. S. Bond and N. M. Smith, *Nucleic Acids Res.*, 2020, **48**, 5766–5776.
46 D.-L. Ma, D. S.-H. Chan, W.-C. Fu, H.-Z. He, H. Yang, S.-C. Yan and C.-H. Leung, *PLoS One*, 2012, **7**, e43278.
47 D. Bhattacharyya, G. M. Arachchilage and S. Basu, *Front. Chem.*, 2016, **4**, 38.
48 J. You, H. Li, X.-M. Lu, W. Li, P.-Y. Wang, S.-X. Dou and X.-G. Xi, *Biosci. Rep.*, 2017, **37**, BSR20170771.
49 J. Carvalho, J. A. Queiroz and C. Cruz, *J. Chem. Educ.*, 2017, **94**, 1547–1551.
50 M. Deiana, J. Jamroskovic, I. Obi and N. Sabouri, *Chem. Commun.*, 2020, **56**, 14251–14254.
51 W. J. Chung, B. Heddi, F. Hamon, M.-P. Teulade-Fichou and A. T. Phan, *Angew. Chem., Int. Ed.*, 2014, **53**, 999–1002.